

ORIGINAL RESEARCH PAPER

Dynamics and Separation-based Adsorption of Binary Mixtures of CH₄, CO₂ and H₂S on MIL-47: GCMC and MD Studies

Abbas Shahsavani^{1,2}, Zohreh Ahadi³, Vahid Sokhanvaran⁴, Maryam Taghizadeh⁵,
Mostafa Hadei⁶, Muhammad Shadman Lakmehsari^{5,*}

¹ Environmental and Occupational Hazards Control Research Center, Shahid Beheshti, University of Medical Sciences, Tehran, Iran.

² Department of Environmental Health Engineering, School of Public Health and safety, Shahid Beheshti University of Medical Sciences, Tehran, Iran.

³ Department of Science and Engineering, Abhar branch, Islamic Azad University, Abhar, Iran.

⁴ Department of Chemistry, Faculty of Basic Sciences, University of Neyshabur, Neyshabur, Iran.

⁵ Department of Chemistry, Faculty of Science, University of Zanjan, P.O.Box 45195-313, Zanjan, Iran.

⁶ Department of Environmental Health Engineering, School of Public Health, Tehran University of Medical Sciences, Tehran, Iran.

Received: 2018-10-20

Accepted: 2018-12-23

Published: 2019-02-01

ABSTRACT

This study aimed to investigate the adsorption of CH₄, CO₂, H₂S at a temperature of 298.15 K and pressure range of 0.1 to 30 atm, and compare the results with experimental data for MIL-47 using GCMC. The maximum CH₄, CO₂ and H₂S adsorptions were 3.6, 10.45, and 12.57 mol.kg⁻¹, respectively. In addition, the selectivity for binary mixtures of CH₄/CO₂ and CH₄/H₂S was calculated. The results for CH₄/CO₂ mixtures at 10 atm showed that: 1) MIL-47 only adsorbed CO₂ in a 0.05 CH₄/0.95 CO₂ mixture, and 2) by increasing the mole fraction of CH₄, the selectivity toward CO₂ decreased. The results for H₂S/CH₄ mixture at 10 atm showed that: 1) H₂S was adsorbed only in mole fractions of 0.95, 0.75, and 0.50 of H₂S, and 2) the observed selectivity was about 132.7 and 63.2 at H₂S mole fractions of 0.25 and 0.05, respectively. The MD simulations and RDF analyses were used to investigate 0.5 CH₄/0.5 CO₂ and 0.75 CH₄/0.25 H₂S mixtures. The results showed that the adsorption mostly occurs on the metallic part of MIL-47. We found that V and O atoms were the active adsorption sites in MIL-47. H₂S and CH₄ showed to have the highest and lowest levels of self-diffusions, respectively. The MD simulations were used to study the self-diffusion for mixtures across all mole fractions. In the binary mixture of 0.95 CO₂/0.05 CH₄, the maximum self-diffusion was 1.49×10⁻¹² m²s⁻¹ for CO₂. The maximum self-diffusion for H₂S in the mixture of 0.05 CH₄/0.95 H₂S was 2.62×10⁻¹⁰ m²s⁻¹.

Keywords: Adsorption; CO₂; H₂S; MIL-47; Selectivity

© 2019 Published by Journal of Nanoanalysis.

How to cite this article

Shahsavani A, Ahadi Z, Sokhanvaran V, Taghizadeh M, Hadei M, Shadman Lakmehsari M. Dynamics and Separation-based Adsorption of Binary Mixtures of CH₄, CO₂ and H₂S on MIL-47: GCMC and MD Studies. J. Nanoanalysis., 2019; 6(1): 48-59. DOI: 10.22034/jna.2019.664503

INTRODUCTION

The use of biogas as a renewable energy for sustainable development of energy and power technology has attracted many scientists and policy interests. Therefore, many investigations

* Corresponding Author Email: shadman@znu.ac.ir

have focused on gas purification processes consist of separation/storage of biogas. Biogas refers to the mixtures of H₂S, CO₂ and CH₄. Typically, CO₂ is the major constituent of biogas, and the concentrations of H₂S and CH₄ depend on the



This work is licensed under the Creative Commons Attribution 4.0 International License.

To view a copy of this license, visit <http://creativecommons.org/licenses/by/4.0/>.

nature of the raw organic materials and the process details [1]. A significant characteristic of biogas is its flammability that is due to the presence of CH₄. Because of pollutant nature of H₂S and CO₂, it is recommended to separate them from the biogas to achieve purified CH₄ [2-6].

Many efforts have been carried out on upgrading biogas to achieve a higher CH₄ content. The process of upgrading or sweetening raw biogas focuses on the removal of impurities such as CO₂, H₂O, and H₂S [1,7-10]. Because of its highly corrosive nature, toxicity, and unpleasant odor, H₂S is typically the first component that is removed. While H₂S removal is needed due to its corrosiveness, the CO₂ removal can be increased the concentration of CH₄ that gives a biogas with a higher calorific value that can be injected into the gas grid. Therefore, reducing CO₂ and H₂S content will significantly improve the quality of biogas [11-15]. Some technologies allow for the concurrent removal of H₂S and CO₂. Among chemical, physical, and biological methods for separation of CO₂ and H₂S from biogas, adsorption-based methods are attractive due to their minimum environmental effects and low cost [2,6, 16-17].

Metal-organics frameworks (MOFs) as nanoporous solids are effective for gas adsorption, storage, selective separation, and molecular recognition [18-23]. MOFs are a new class of nanoporous crystalline materials with hybrid inorganic/organic solids and structures that are composed of clusters of a few metal atoms or metal oxide molecules in a three-dimensional structure by interconnected rigid or semi-rigid organic linkers [19-20,24].

Due to the presence of H₂S in the biogas, it is important to find new nanoporous solid media with the ability to remove or adsorb H₂S. To find the best candidates from thousands of possible MOFs, a theoretical analysis of properties such as internal MOFs' surface area can be performed for CO₂ and H₂S, and the results can be compared with the experimental data in an efficient manner.

THEORETICAL and EXPERIMENTAL RESOURCES

Several investigations have theoretically or experimentally studied the adsorption of pure CO₂ [8-9,25-28], H₂S [12,16], and CH₄ [25-28] and their binary mixtures: CO₂/CH₄ [14,26-30] and H₂S/CH₄ [17,29] in a variety of nanostructures.

Lu et al.[28] have shown that carbon foam nanostructures have the highest adsorption

capacity for CO₂ (1–3.5 mmolkg⁻¹ at 0.01–6.0 MPa) and CH₄ (0.25–0.5 mmolkg⁻¹ at 0.01–6.0 MPa). Furthermore, they found that the highest selectivity (~80) is related to modified carbon nanotubes, especially at low pressures (0.01 MPa) [28]. Llewellyn et al. studied the uptakes of CO₂ and CH₄ in MIL-100 and MIL-101. The best sample, MIL-101c, exhibited the highest loading of CO₂ with a capacity of 40 mmolkg⁻¹ at 5 MPa [25]. Separation of biogas consisting of CH₄, CO₂, and H₂S by single-walled CNTs using Grand Canonical Monte Carlo (GCMC) simulation have been studied at various temperatures (288–338 K) and 0.1 and 1 MPa, and the selectivity of H₂S/CH₄ and CO₂/CH₄ have been determined [29]. It is illustrated that despite lower concentration of CO₂ than CH₄ and trace levels of H₂S in biogas, the CNTs can be effective tools in CH₄ separation from biogas [29]. Loading amounts of CH₄, CO₂ and H₂S in (10,10) CNT bundles at 298 K and 100 kPa were achieved to be 1.652, 3.8097, and 3.6177, respectively; while for (6,6) CNT bundles, they were 1.790, 1.960 and 1.856, respectively. In addition, H₂S/CH₄ and CO₂/CH₄ selectivity in (10,10) CNT bundles at 298 K and 100 kPa were calculated to be 12.156 and 3.384, respectively; while their values were 40.22 and 4.00 for (6,6) CNT bundles, respectively [29]. In another study, Herm et al. used Mg₂(DOBDC) and reported that the absolute adsorption of CO₂ and CH₄ at 313 K and 35 MPa were about 14 and 9 molkg⁻¹, respectively. In addition, the selectivity for 1:1 CO₂/CH₄ was a little lower than 125 [26].

In another study, the separation based on the adsorption of CH₄/CO₂ mixture was studied using a fixed-bed packed with MIL-53(Al) pellets in breakthrough experiments at pressures between 1 and 8 bar and different mixture compositions. The selectivity at the pressures below and above 5 bar was 7 and 4, respectively [14]. In another study, the adsorption of CO₂ and CH₄ in a mixed-ligand MOF Zn₂(NDC)₂(DPNI) [NDC =2,6-naphthalenedicarboxylate, DPNI = N,N'-di-(4-pyridyl)-1,4,5,8-naphthalene tetracarboxydiimide] were studied by volumetric adsorption calculations using GCMC simulations and experimental efforts using the ideal adsorbed solution theory (IAST) for the single-component CO₂ and CH₄, and binary mixture adsorption. Experiment section was shown a selectivity of ~30 for CO₂ over CH₄, which is among the highest selectivity values reported for this separation. In addition, GCMC simulations were in a good agreement with IAST results for both

single-component and mixture adsorption [30]. In another study, Gilani et al. experimental separation of H₂S from H₂S/CH₄ mixture using functionalized and non-functionalized vertically aligned carbon nanotube (CNT) membranes [17]. The selectivity of CNTs with internal diameters of 23 and 8 nm to separate H₂S from CH₄ was obtained to be in the ranges of 1.36–1.58 and 2.11–2.86, respectively. Also, the selectivity for amido-functionalized CNT membrane was in the range of 3.0–5.57 [17].

There are many molecular models of CH₄, CO₂ and H₂S used in molecular simulations. The main objective of this study is to find the best molecular model for each gas in a way that the findings are in agreement with experimental results. The MIL-47 was selected for this study, because of its use in theoretical and experimental investigations in order to adsorb and separate CH₄, CO₂ and H₂S selectively.

Adsorption of CH₄ and CO₂ on MIL-47 has been frequently investigated [8,27,31]. Liu and Smit reported the CO₂ adsorption capacity of 9.7 molkg⁻¹ in MIL-47(V) applying GCMC simulation at 304 K and 2.0 MPa [8]. Ramsahye et al. obtained an absolute CO₂ adsorption of 10.82 molkg⁻¹ at 303 K and 10.19 atm using MIL-47(V) [9]. Leus was reported the adsorption of CO₂ and CH₄ on MIL-47 [27]. Isotherms of adsorption of pure CO₂ and CH₄ at 30°C were obtained using volumetric method. The results showed that the adsorption of CO₂ and CH₄ were 7.7 and 4.1 mmolkg⁻¹, respectively, that were lower than the corresponding values of 10.1 and 5.5 mmolkg⁻¹ reported in another study [31]. This difference is probably due to the differences in sample preparation methods and nano-porous size. In fact, the nano-porous size in Leus [27]

and Bourrelly's studies were 0.4 and 0.46 mlg⁻¹, respectively [27,31].

In another study, Hamon et al. studied the adsorption of H₂S in some MILs at room temperature. They observed that H₂S adsorption on the large-pores MIL-100 and MIL-101 is partially irreversible on experimental conditions, while the adsorption occurred perfectly reversible in the small-pores MIL-47(V) and MIL-53(Al,Cr), [12]. Hamon et al. explored the adsorption of H₂S in both MIL-47(V) and MIL-53(Cr) by combining infrared measurements and molecular simulations. The MIL-47(V) structure remained rigid up to a pressure of 1.8 MPa, while the MIL-53(Cr) structure transitioned from the narrow pore version (NP) at very low pressure to the large pore (LP) at higher pressure (1.8 MPa). Both experimental and simulated adsorption enthalpies for H₂S decreased in the following sequence: MIL-53(Cr) NP > MIL-47(V) > MIL-53(Cr) LP [16]. As a result, it can be stated that MIL-47(V) is a good option for the purification of a gas mixture containing H₂S [12].

CHEMICAL STRUCTURE of MIL-47

Therefore; one of the most suitable nanoporous solids media for H₂S adsorption is V^(IV)(O) (BDC) (MIL-47(V)) [V^(IV) = vanadium (4+), and BDC is ligand = the benzene dicarboxylic (O₂C-C₆H₄-CO₂) [31], and MIL = Materials of Institute Lavoisier] [19] that it is a member of the category of MOFs [12]. This solid is preserved anhydrous at room temperature. Firstly, it is typically built up from VCl₃ and terephthalic acid that are mixed together with deionized H₂O and transferred to a Teflon-lined stainless autoclave for 4 days at 200°C.

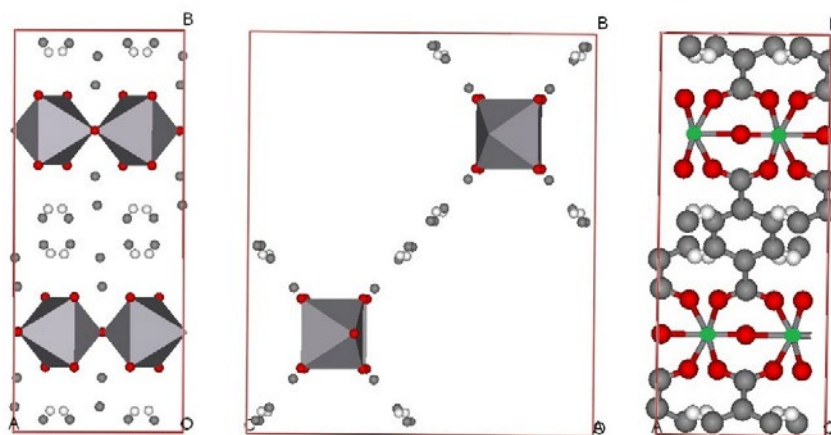


Fig. 1. Chemical cell structure of MIL-47(V). The left and middle hands show polyhedron of cluster and the right hand is based on ball and stick format. Grey, white, red and green atoms are C, H, O and V, respectively.

Then, the as-synthesized MIL-47 has been filtered, washed with acetone, and calcined. This procedure was developed by Barthelet et al in 2001 [32]. The chemical-spatial structure of MIL-47 is constructed from infinite chains of corner-sharing with a center of V^{IV} that it is coordinated by the dicarboxylate groups. This topological structure exhibit three-dimensional orthorhombic large nano-pores that form long tunnels. Each tunnel has four walls and eight corners. In each corner, a V^{IV}O₆ octahedra cluster can be observed that four oxygen atoms are from four carboxylate groups, and two other oxygen atoms are on the O–V–O axis, while the corners are further inter-connected by the carboxylate linkers that make four walls of benzyl units [1,31]. Fig. 1 shows the carboxylate linker and a node of MIL-47. Surface area, pore volume and pore diameter of MIL-47 are 600-1225 m²g⁻¹, 0.4 cm³g⁻¹, and <2 nm, respectively [13,31].

According to the above short review on separation-based adsorption of CO₂ and H₂S in binary mixtures with CH₄, the significant part of our study is concerned with elimination of CO₂ and H₂S from CH₄ in their binary mixtures (CO₂/CH₄ and H₂S/CH₄) by applying molecular simulation [11]. The next section describes the molecular simulation method and details that have applied in our study.

SIMULATION METHOD AND DETAILS

The GCMC simulations were applied to calculate absolute and excess adsorption of i) pure components at 298.15 K and pressure range of 0.1-30 atm, and ii) CO₂/CH₄ and H₂S/CH₄ binary

mixtures to MIL-47. The bulk composition in both binary mixtures were 5:95, 25:75, 50:50, 75:25 and 95:5 at 298.15 K and 10 atm. The multi-propose Simulation Code (MuSiC) of molecular simulation package was used for all GCMC simulations [33]. The GCMC simulation box consisted of 16 (2×2×4) unit cells for the orthorhombic MIL-47(V) structure. MIL-47(V) was treated as a rigid framework, with atoms frozen at their crystallographic positions during the simulations, except for hydrogen atoms that optimized by PBC-DFT calculation. However, H-optimization was done on a unit cell with 1152 atoms within GGA using the exchange correlation functional of Perdew–Burke–Ernzerhof (PBE) [34] that was sampled by 1×1×1 *k*-points. We used the pseudo-potential to produce double- ζ polarized (DZP) basis set to use SIESAT quantum chemical package [35-36]. In addition, partial charges for atoms of MIL-47 were obtained by the PBC-DFT calculations using Mulliken charge partitioning method (Fig. 2).

During the GCMC simulation, the PBC was used in three dimensions (x, y, and z directions), and the electrostatic contributions were estimated using the WOLF summation. The short-range interactions were truncated at a cut-off distance fixed at 13.435 Å. We considered the last half of 4×10⁶ moves for calculating ensemble averages of thermodynamics parameters for each run.

Lennard-Jones (LJ) parameters for atoms of MIL-47 framework were taken from the DREIDING [37] force field if available, otherwise from the UFF force field [38]. Additionally, we modeled hydrogen sulfide (H₂S) using a three-

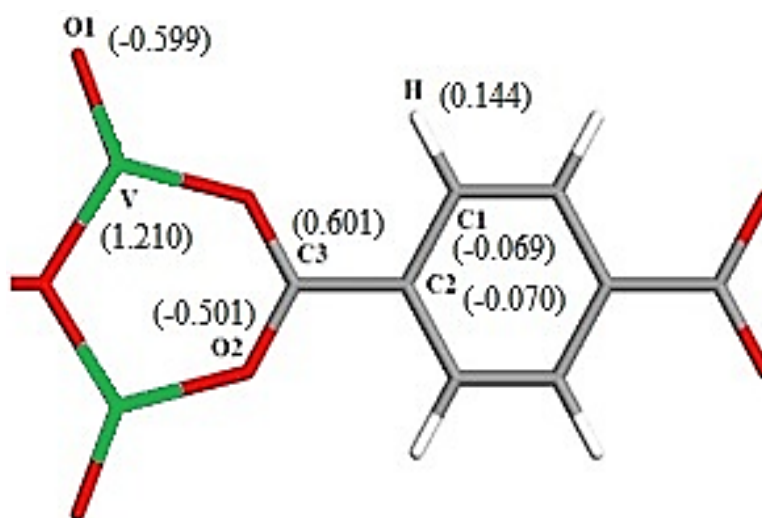


Fig. 2. The partial charges for atoms of MIL-47 obtained and used in this study

site model, in which interaction sites are placed at each of the hydrogen (H) and sulfur (S) atom nuclei model reported previously [39]. ϵ/k_B , σ and q for S were 250.0 K, 3.72 Å and -0.248 e , and for H were 3.9 K, 0.98 Å and 0.124 e , respectively. The S-H bond length was 0.1365 nm, and the angle of H-S-H was 91.5°. In addition, the carbon dioxide (CO₂) was modeled as a rigid linear triatomic molecule with three charged LJ interaction sites located at each atom. The LJ potential parameters were $\sigma_O=0.305$ nm and $\epsilon/k_B=79.0$ K for atom O and $\sigma_C=0.280$ nm and $\epsilon/k_B=27.0$ K for atom C with a C-O bond length of $l=0.116$ nm. Partial point charges centered at each LJ site were $q_O=-0.35e$ and $q_C=0.70e$, and were taken from the TraPPE force field [40]. Methane (CH₄) was simulated by the five-site model with LJ interaction, reported previously by Terzyk [41]. ϵ/k_B , σ and q for C were 55.055 K, 3.40 Å and -0.66 e and for H were 7.901 K, 2.65 Å and 0.165 e , respectively. The bond length and H-C-H angle were 1.09 Å and 109°:28', respectively.

It should be noted that we investigated the excess adsorption, and compared the results with experimental data. The absolute amount was defined as the total amount of gas contained in the pores. The excess amount was calculated as the absolute amount minus the amount of gas that would be present in the pores in the absence of gas-solid intermolecular forces [42].

The last parameter which considered on GCMC part is the selectivity factor that is shown as follow equation: $S = \frac{q_1/q_2}{p_1/p_2}$.

Where S is the selectivity factor, q_i represents the adsorbed quantity of component i , and p_i represents the partial pressure of component i [43].

In the next step, the equilibrium molecular dynamics (EMD) simulation was performed to investigate the dynamical behavior of gases in MIL-47 at 298 K. The DL_POLY package was used for all MD simulations [45]. In statistical mechanics, the radial distribution function (RDF, i.e. pair correlation function) $g(r)$ in a system of particles (atoms, molecules, colloids, etc.) describes how density varies as a function of distance from a reference particle. Therefore, we calculated the pair correlation between guest atom and host framework. The Nosé-Hoover thermostat, in canonical ensemble (NVT) and Verlet equation of motion with Ewald summation method for considering electrostatic interactions with a length simulation of 0.1 to 3 ns, and time step of 1 fs were applied in EMD simulations. The MD simulations for calculations of RDF analysis and self-diffusions (D_s) were used to study 0.5 CH₄/0.5 CO₂, 0.75 CH₄/0.25 H₂S mixtures. RDFs were plotted to understand each atom of the molecule adsorbs around which atoms of the framework, and show that the adsorption mostly occurs at which part of MIL-47. The input of any MD was the same outputs of the corresponding GCMC that were considered without any change of thermodynamic conditions. This means that the temperature, pressure and force fields used in MD were unchanged from GCMC.

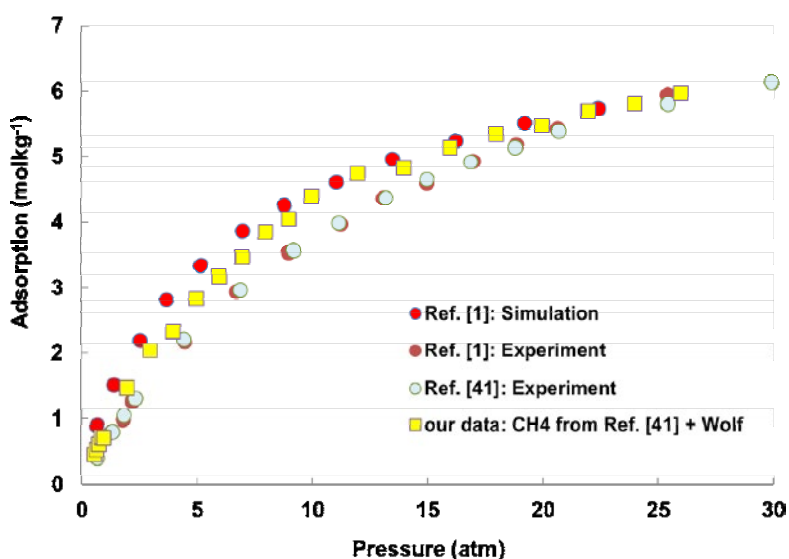


Fig. 3. The simulated methane adsorption on MIL-47 and comparison with simulation [1] and experimental data [1,41] from other studies.

RESULTS AND DISCUSSION

Adsorption Isotherms

To confirm the reliability of the force field adopted in this work, the adsorption isotherms for CH₄, CO₂ and H₂S adsorbed to MIL-47 were calculated using GCMC simulation. Adsorption of these various gases to MIL-47 was simulated, and compared to experimental data to test the validity of proposed atomic models. The results of methane simulations and the comparisons with simulations and experimental data published in other studies are presented in Fig. 3.

According to Fig. 3, the simulated methane

adsorption isotherm in this study is reasonably in good agreement with the experimental data reported in a previous study [1]. The maximum value for CH₄ adsorption was 6.08 molkg⁻¹ that is in similar to experimental data (6.1 molkg⁻¹ at Ref. [41]).

For investigation of charge effect on adsorption, we simulated the carbon dioxide adsorption isotherm on MIL-47 using Ewald and Wolf algorithms (See Fig. 4). Simulations of CO₂ adsorption were performed to compare against experimental data from the literature [13,27]. It should be noted that in all simulations, the pure

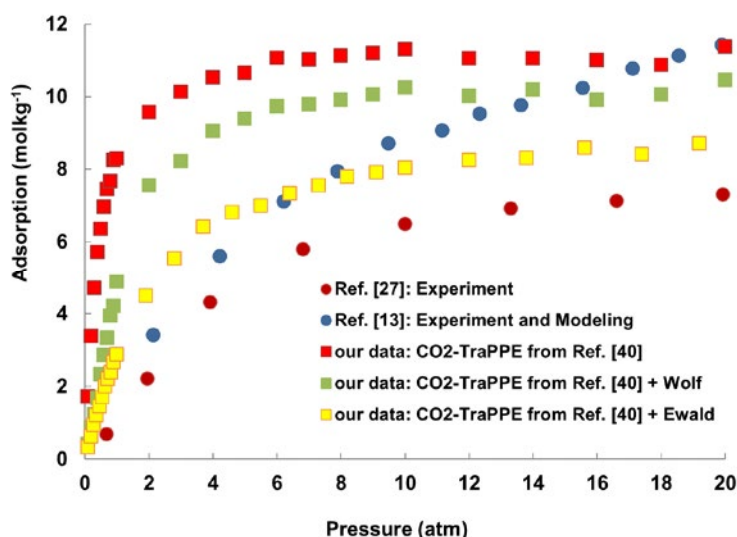


Fig. 4. The simulated CO₂ adsorption on MIL-47 and comparison with experimental and modeling findings from other studies [13,27].

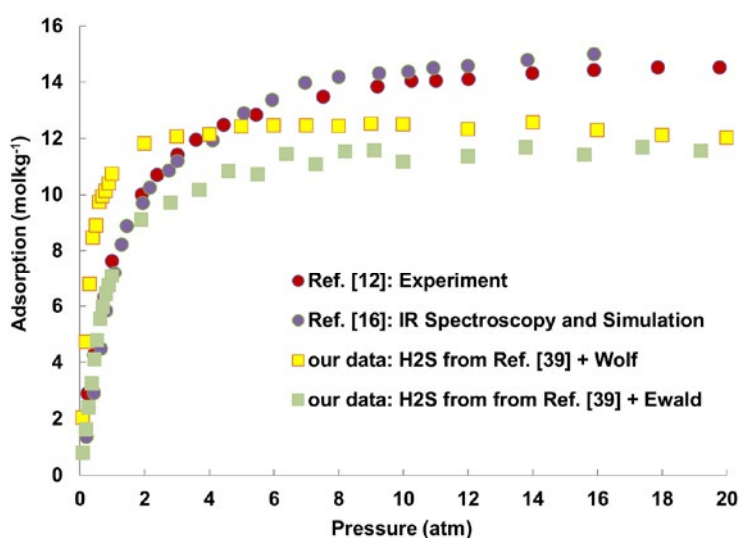


Fig. 5. The H₂S adsorption on MIL-47 and comparison with experimental and modeling results from other studies [12,16].

gas adsorption using Mulliken and CHELPG charges for MIL-47's atoms were investigated, and the results showed that the Mulliken charge is in a reasonable agreement with the experimental data. Results of CO₂ adsorption using Ewald algorithm are more similar to experimental data reported in Ref. [27] than Wolf algorithm. The maximum value of CO₂ adsorption on MIL-47 was 8.7 molkg⁻¹ at 19.93 atm; while, its experimental value was 7.3 molkg⁻¹.

The calculated adsorption isotherms of H₂S adsorption on MIL-47 at 298 K and pressures up to 20 atm are presented in Fig. 5.

It can be observed from this Figure that only at low pressures (<2 atm), the simulated hydrogen sulfide adsorption isotherm is in a good agreement with the experimental isotherms of two previous studies [12,16]. Additionally, the adsorption results obtained by the Wolf algorithm are closer to the experimental values in moderate pressures. The maximum values of simulated adsorption of H₂S were 12.57 and 11.68 molkg⁻¹ at 14 atm for Wolf and Ewald summation, respectively.

Separation of CO₂ and H₂S from CH₄

To further investigate the selective adsorption properties of MIL-47, and explore its potential application in industrial processes, binary mixtures of CO₂/CH₄ were prepared, and undergone the experimental analyses. The calculated CO₂/CH₄ selectivity of MIL-47 for adsorption of five mole fraction mixtures at 0 to 30 atm is depicted in Fig. 6. According to this Figure, the selectivity of CO₂/CH₄ increases monotonically with increasing pressure, and gradually approaches a constant. By increasing the mole-fraction of CH₄, the CO₂/CH₄ selectivity decreases due to the fact that the interaction of CO₂ molecules with the atoms of MOF structure is stronger than that with CH₄ molecules. In addition, maximum selectivity of CO₂ comparing to methane with a mole fraction of 0.05 CH₄/0.95 CO₂ was almost 155.38 at 20 atm. The Coulombic and non-Coulombic interactions of CO₂ and CH₄ with MIL-47 in binary mixtures are given in Table 1.

According to Table 1, the non-Coulombic effect is greater than Coulombic interaction. In addition,

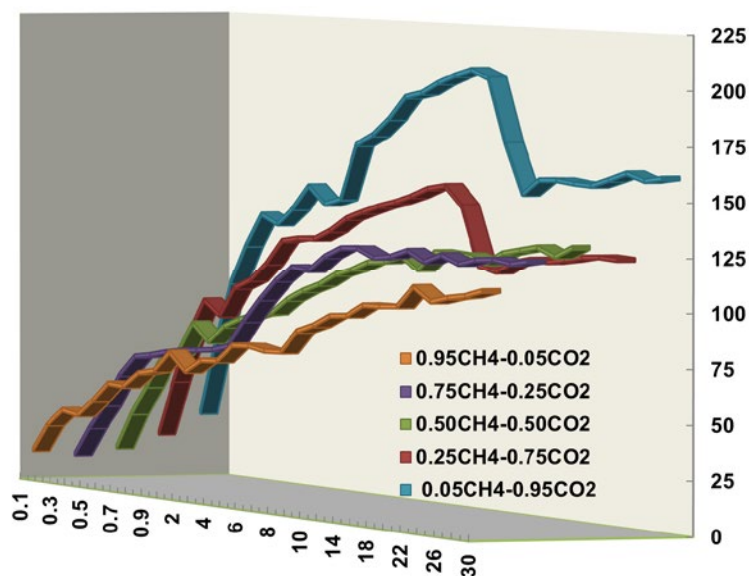


Fig. 6. Adsorption selectivity of CO₂/CH₄ (mole fractions: 0.95/0.05, 0.75/0.25, 0.50/0.50, 0.25/0.75, 0.05/0.95) on MIL-47

Table 1. Interactions of CO₂ and CH₄ in CO₂/CH₄ mixture with MIL-47

mole fraction	CH ₄ - MIL-47		CO ₂ - MIL-47	
	Coulombic (kJmol ⁻¹)	Non-Coulombic (kJmol ⁻¹)	Coulombic (kJmol ⁻¹)	Non-Coulombic (kJmol ⁻¹)
0.05 CH ₄ - 0.95 CO ₂	-0.34540	-13.15473	-2.30010	-16.80958
0.25 CH ₄ - 0.75 CO ₂	-0.18346	-12.84491	-2.56105	-16.70508
0.5 CH ₄ - 0.5 CO ₂	-0.29178	-13.30637	-2.67667	-16.81725
0.75 CH ₄ - 0.25 CO ₂	-0.28456	-13.05461	-3.26648	-16.72038
0.95 CH ₄ - 0.05 CO ₂	-0.31557	-13.01774	-3.07133	-16.88455

non-Coulombic and Coulombic interactions of CO₂ molecules with MOF atoms are greater than those for methane.

The adsorption selectivity of the 5 mole fractions of H₂S/CH₄ mixture on MIL-47 in the pressure range of 0-30 atm is plotted in Fig. 7. This Figure shows that the simulated H₂S/CH₄ selectivity in all of mole-fractions increases with increasing pressure, except for 0.95 CH₄/0.05 H₂S. This is because the interactions of H₂S with MIL-47 atoms is higher than those for CH₄. The maximum values for H₂S/CH₄ selectivity is 190.58 at 26 atm in 0.50/0.50 mole-fraction of H₂S/CH₄ mixture. The Coulombic and non-Coulombic interaction of CH₄ and H₂S with MIL-47 in H₂S/CH₄ mixture are presented in Table 2. According to Table 2, in the H₂S/CH₄ mixture, the effect of non-Coulombic is greater than Coulombic interaction. In addition, the non-Coulombic and Coulombic interactions of H₂S molecules with MIL-47 framework's atoms are greater than those for CH₄.

MIL-47's CHARGE EFFECT ON SELECTIVITY

In order to investigate the effect of charge on selectivity, we calculated the studied selectivity

using CHELPG and Mulliken charges. The selectivities of CO₂/CH₄, H₂S/CH₄ and H₂S/CO₂ are presented in Fig. 8 (A-C). As shown in Fig. 8 A, in 0.05, 0.25, 0.50 and 0.75 mole-fractions of CH₄, the CO₂/CH₄ selectivity is infinite (empty spaces in figure represent CHELPG charge). In case of CHELPG charge, only in lowest mole fraction of CO₂ (0.05 CO₂/0.95 CH₄), the CO₂/CH₄ selectivity was slightly lower, but it was still more than that for Mulliken charge. In case of H₂S/CH₄ selectivity, similar results were obtained. In Fig. 8 C, it can be observed that there was almost a decreasing trend while using CHELPG charge at simulation. Therefore H₂S/CO₂ selectivity decreases using CHELPG charge.

RADIAL DISTRIBUTION FUNCTION (RDF)

In this part, the binary interaction between host gases and guest framework are exhibited as RDF plot according to distances between the atoms interest gas and guest.

RDF for CO₂/CH₄

In order to calculate RDF for CO₂/CH₄, the 0.50/0.50 mole-fraction was considered. It should

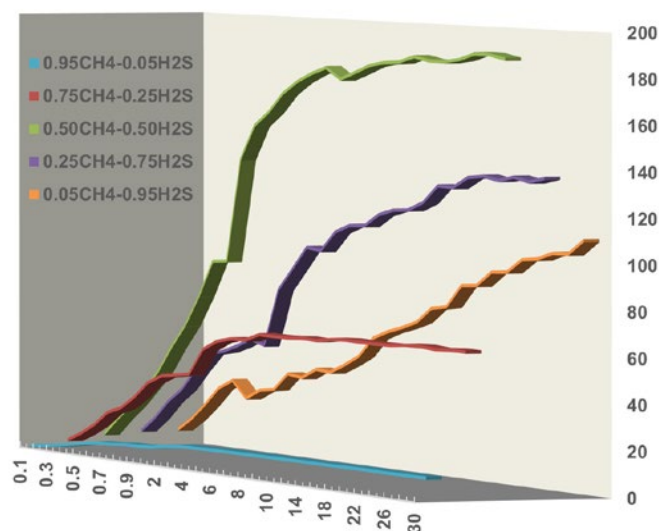


Fig. 7. Adsorption selectivity of H₂S/CH₄ (mole fractions: 0.25/0.75, 0.50/0.50, 0.75/0.25, 0.05/0.95, 0.95/0.05] on MIL-47

Table 2. Interaction of CH₄ and H₂S in CH₄/H₂S mixture with MIL-47 framework

mole fraction	CH ₄ - MIL-47		H ₂ S - MIL-47	
	Coulombic (kJmol ⁻¹)	Non-Coulombic (kJmol ⁻¹)	Coulombic (kJmol ⁻¹)	Non-Coulombic (kJmol ⁻¹)
0.05 CH ₄ - 0.95 H ₂ S	-0.35689	-13.11599	-2.00932	-19.07625
0.25 CH ₄ - 0.75 H ₂ S	-0.19301	-13.39732	-2.00724	-19.18141
0.5 CH ₄ - 0.5 H ₂ S	-0.43031	-13.84212	-2.07247	-19.18558
0.75 CH ₄ - 0.25 H ₂ S	-0.44220	-13.76447	-2.46466	-19.11430
0.95 CH ₄ - 0.05 H ₂ S	-0.30019	-13.30506	-3.79579	-19.09562

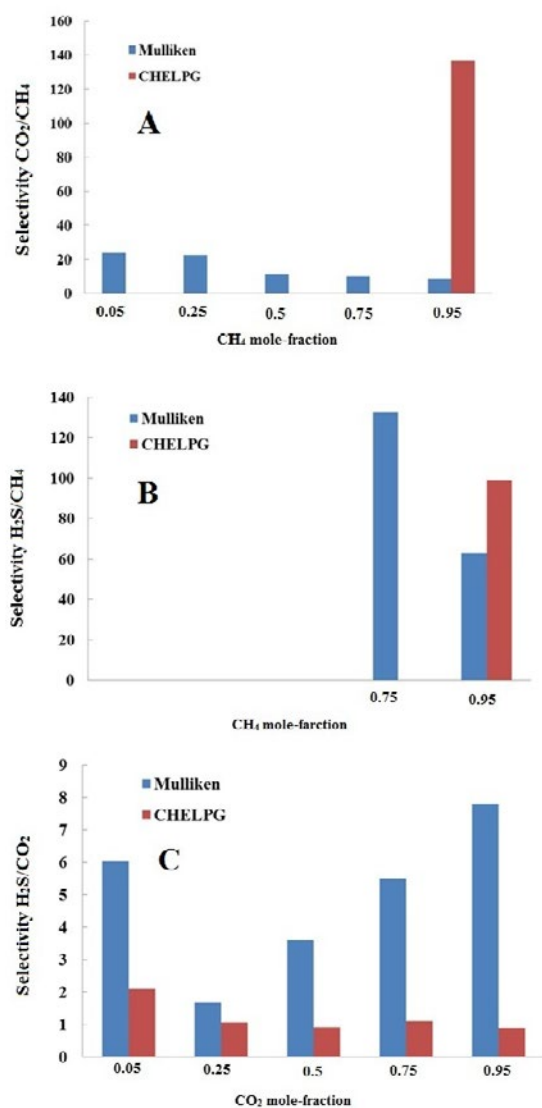


Fig. 8. Effect of atomic charge of MIL-47 on the A) CO₂/CH₄, B) H₂S/CH₄, and C) H₂S/CO₂ selectivity

be noted that this mixture had a good selectivity. Fig. 9 presents the RDF plot between O and C atoms from CO₂ and C and H atoms from CH₄ with V and O1 from MIL-47.

This figure shows that the most interaction parts in MIL-47 with host molecules are distributed on its two parts. O (CO₂) and C (CH₄) tend to interact with the metal part of MIL-47 i.e. V. In addition, C (CO₂) and H (CH₄) tend to interact with the linker part of MIL-47 i.e. O1. This is possibly due to the role of interactions between host and guest atoms. The potential role was divided into two sections. The interatomic potential obtained from Lorentz-Berthelot mixing rule (short-range interaction) and Coulombic interactions (long-range interaction) between atoms of host and guest. Furthermore, another reason is maybe related to the open-metal site of MIL-47 metal part (V). O (CO₂) has two lone-pairs and *d*-orbital of V is almost empty. However, Newtonian molecular simulation cannot predict the electronic interactions, while this role was absolutely considered in calculation of potential depth of each atom. Therefore, V with maximum atomic positive charge and empty *d*-orbital, and O1 as the maximum atomic negative charge prone to have considerable interactions. The self-diffusions of CO₂ and CH₄ inside MIL-47 were calculated to be 8.58×10⁻⁴ and 1.456×10⁻⁴ (10⁻⁹m²s⁻¹), respectively. This emphasizes that due to higher potential depth and atomic charge of CO₂ comparing to CH₄, it can interact with MIL-47, and be adsorbed and separated from binary mixture.

RDF for H₂S/CH₄

In order to calculate RDF for H₂S/CH₄, the 0.75/0.25 mole-fraction of this mixture was considered. Fig. 10 presents the RDF plot between

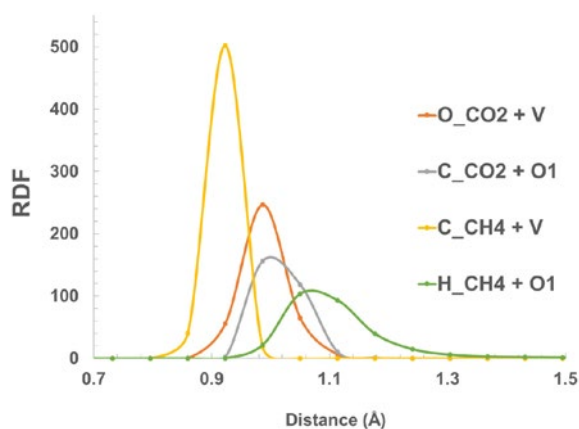


Fig. 9. RDF plot between CO₂ and CH₄ atoms with V and O1 atoms (MIL-47)

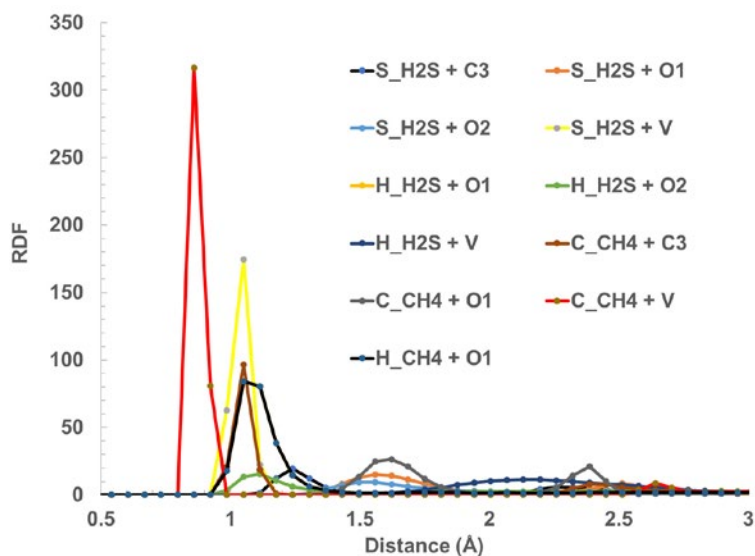


Fig. 10. RDF plot between H₂S and CH₄'s atoms with MIL-47's atoms.

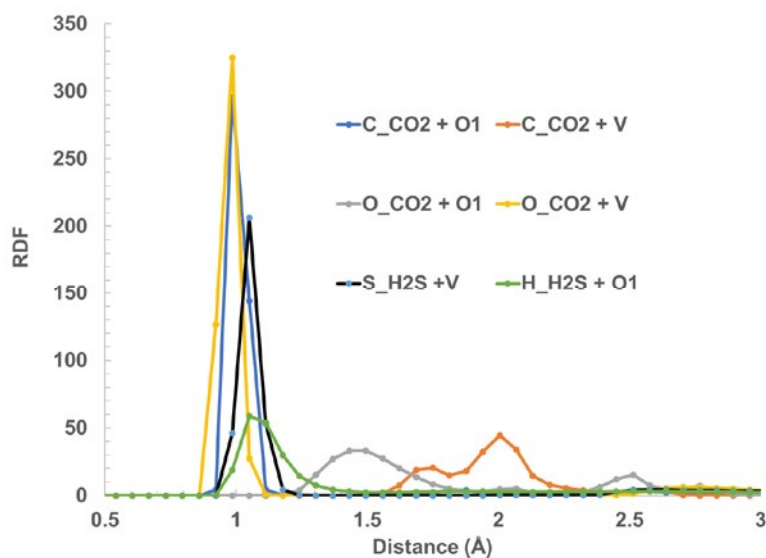


Fig. 11. The RDF plot between H₂S and CO₂'s atoms with MIL-47's atoms

H and S from H₂S and C and H from CH₄ with MIL-47's atoms.

Fig. 10 shows that both organic linker and cluster parts of MIL-47 had an important role with interaction to H and S atoms from H₂S and H and C atoms from CH₄. C (CH₄) and S (H₂S) interact with V (MIL-47) more than other pairs. Additionally, these atoms [C (CH₄) and S (H₂S)] also interact with C3 (from organic linker part of MIL-47). H (H₂S) and O2 (from organic linker part of MIL-47)

have a weak interaction. H and C from CH₄ interact with O1 (from organic linker part of MIL-47) at 1.25 and 1.6 Å, respectively. The self-diffusions of H₂S and CH₄ inside MIL-47 were calculated to be 0.1145 and 2.35 × 10⁻³ (10⁻⁹ m² s⁻¹), respectively. It should be considered that S in H₂S is very similar to O in CO₂, and have two lone-pairs. C3 is the second atom in terms of positive charge after V in MIL-47 atoms. O1 has the maximum negative charge. The potential depth interaction of H₂S is more than

CH₄. From all the above, one can conclude that H₂S tend to have a dynamical behavior around V as open-metal site and C3 as organic linker part of MIL-47; while, CH₄ was found around V, O1 and C3. However, due to more self-diffusion and dynamics of H₂S comparing to CH₄, it can be found around V in lower levels.

RDF for H₂S/CO₂

The RDF for H₂S/CO₂ at the 0.50/0.25 mole-fraction was calculated. Fig. 11 presents the RDF plot between H and S from H₂S and C and O from CO₂ with MIL-47's atoms. Fig. 11 clearly demonstrates that S (H₂S) and O (CO₂) had more interaction with V, due to the reasons stated previously. In addition, C (CO₂) and H (H₂S) interacted with O1 (from organic linker part of MIL-47). The self-diffusion for H₂S and CO₂ inside MIL-47 were 1.8×10^{-2} and 2.0×10^{-3} ($10^{-9} \text{m}^2 \text{s}^{-1}$), respectively. Therefore, due to more self-diffusion for H₂S than CO₂, it can stay around V less.

CONCLUSION

We found that the GCMC simulation is able to describe the adsorption behavior of H₂S, CO₂ and CH₄ in MOFs. Our results revealed that gas adsorption on MIL-47 follow as; H₂S > CO₂ > CH₄, due to the interaction with atoms of MOF structure. The CO₂/CH₄ and H₂S/CH₄ selectivity was in an appropriate level, due to the strong interaction of CO₂ and H₂S with atoms of MIL-47 framework. The MD simulations were used to study structural and dynamical properties. The RDFs plots indicated that the suitable sites for adsorption of gas on MIL-47 is metal sites, and then C3 atom of organic linker that connects two oxygen atoms. In addition, our MD results predicted that H₂S can stay around V (MIL-47) less, because the diffusion coefficients of H₂S are more than those for CO₂ and CH₄ in their binary mixtures (H₂S/CH₄ and H₂S/CO₂).

ACKNOWLEDGEMENTS

The authors wish to thank Shahid Beheshti University of Medical Sciences with grant number #5075. We also, thank the Environmental and Occupational Hazards Control Research Center for supporting grant number #7333.

CONFLICT OF INTEREST

The authors declare that there is no conflict of interests regarding the publication of this manuscript.

REFERENCES

- [1] N. Rosenbach, H. Jobic, A. Ghoufi, F. Salles, G. Maurin, S. Bourrelly, et al., *Angew. Chemie - Int. Ed.* 47, 6611–6615 (2008).
- [2] N. Tippayawong, P. Thanompongchart, *Energy* 35, 4531–4535 (2010).
- [3] R. Krishna, *RSC Adv.* 5, 52269–52295 (2015).
- [4] S. D. Kenarsari, D. Yang, G. Jiang, S. Zhang, J. Wang, A. G. Russell, et al., *RSC Adv.* 3, 22739 (2013).
- [5] X. Chen, H. Vinh-Thang, A. A. Ramirez, D. Rodrigue, S. Kaliaguine, *RSC Adv.* 5, 24399–24448 (2015).
- [6] A. Nakarmi, A. B. Karki, et al. *Biogas As Renewable Source of Energy in Nepal, Theory and Development*, Alternative Energy Promotion Centre, 2005.
- [7] G. Maurin, S. Bourrelly, P.L. Llewellyn, R.G. Bell, *Microporous Mesoporous Mater.* 89, 96–102 (2006).
- [8] B. Liu, B. Smit, *Langmuir* 25, 5918–26 (2009).
- [9] N. A. Ramsahye, G. Maurin, S. Bourrelly, P.L. Llewellyn, T. Devic, C. Serre, et al., *Adsorption* 13, 461–467 (2007).
- [10] G. Maurin, P.L. Llewellyn, R.G. Bell, *J. Phys. Chem. B.* 109, 16084–16091 (2005).
- [11] N. Heymans, S. Vaesen, G. De Weireld, *Microporous Mesoporous Mater.* 154, 93–99 (2012).
- [12] L. Hamon, C. Serre, T. Devic, T. Loiseau, F. Millange, G. Férey, et al., *J. Am. Chem. Soc.* 131, 8775–8777 (2009).
- [13] A. O. Yazaydin, R.Q. Snurr, T.-H. Park, K. Koh, J. Liu, M.D. Levan, et al., *J. Am. Chem. Soc.* 131, 18198–9 (2009).
- [14] V. Finsy, L. Ma, L. Alaerts, D. E. De Vos, G. V. Baron, J.F.M. Denayer, *Microporous Mesoporous Mater.* 120, 221–227 (2009).
- [15] H. Huang, W. Zhang, D. Liu, C. Zhong, *Ind. Eng. Chem. Res.* 51, 10031–10038 (2012).
- [16] L. Hamon, A. Ghou, L. Oliviero, A. Travert, J. Lavalley, T. Devic, et al., *J. Phys. Chem. C.* 53, 2047–2056 (2011).
- [17] N. Gilani, J. Towfighi, A. Rashidi, T. Mohammadi, M.R. Omidkhan, A. Sadeghian, *Appl. Surf. Sci.* 270, 115–123 (2013).
- [18] B. Li, H. Wang, B. Chen, *Chem. - An Asian J.* 9, 1474–1498 (2014).
- [19] J. Li, J. Sculley, H. Zhou, *Chem. Rev.* 112, 869–932 (2012).
- [20] S. Kitagawa, R. Matsuda, *Coord. Chem. Rev.* 251, 2490–2509 (2007).
- [21] Hadei, M., Hopke, P. K., Nazari, S. S. H., Yarahmadi, M., Shahsavani, A., & Alipour, M. R. Estimation of mortality and hospital admissions attributed to criteria air pollutants in Tehran metropolis, Iran (2013–2016). *Aerosol Air Qual Res.* 17, 2474–2481 (2017).
- [22] T. Asadi, M.R. Ehsani, a. M. Ribeiro, J.M. Loureiro, A. E. Rodrigues, *Chem. Eng. Technol.* 36, 1231–1239 (2013).
- [23] D.I. Kolokolov, H. Jobic, a. G. Stepanov, M. Plazanet, M. Zbiri, J. Ollivier, et al., *Eur. Phys. J. Spec. Top.* 189, 263–271 (2010).
- [24] Massoudinejad, M., Ghaderpoori, M., Shahsavani, A., Jafari, A., Kamarehie, B., Ghaderpoury, A., & Amini, M. M. Ethylenediamine functionalized cubic ZIF-8 for arsenic adsorption from aqueous solution: Modeling, isotherms, kinetics and thermodynamics. *Journal of Molecular Liquids*, 255, 263–268 (2018).
- [25] P.L. Llewellyn, S. Bourrelly, C. Serre, A. Vimont, M. Daturi, L. Hamon, et al., *Langmuir* 24, 7245–7250 (2008).
- [26] Z.R. Herm, R. Krishna, J.R. Long, *Microporous Mesoporous Mater.* 157, 94–100 (2012).

- [27] K. Leus, M. Vandichel, Y. Y. Liu, I. Muylaert, J. Musschoot, S. Pyl, H. Vrielinck, F. Callens, G. B. Marin, C. Detavernier, P. V. Wiper, Y. Z. Khimyak, M. Waroquier, V. Van Speybroeck, P. Van Der Voort, *Journal of Catalysis*, 285, 196–207 (2012).
- [28] L. Lu, S. Wang, E. a. Müller, W. Cao, Y. Zhu, X. Lu, et al., *Fluid Phase Equilib.* 362, 227–234 (2014).
- [29] S. Yeganegi and F. Gholampour, *Acta Chim. Slov.* 59, 888–896 (2012).
- [30] Y. Bae, K.L. Mulfort, H. Frost, P. Ryan, S. Punnathanam, L.J. Broadbelt, et al., *Langmuir* 24, 8592–8598 (2008).
- [31] S. Bourrelly, P.L. Llewellyn, C. Serre, F. Millange, T. Loiseau, G. Férey, *J. Am. Chem. Soc.* 127, 13519–21 (2005).
- [32] K. Barthelet, J. Marrot, D. Riou, G. Férey, *Angew. Chemie - Int. Ed.* 41, 281–284 (2002).
- [33] A. Gupta, S. Chempath, M.J. Sanborn, L.A. Clark, R.Q. Snurr, *Mol. Simul.* 29, 29–46 (2003).
- [34] J. P. Perdew, K. Burke, M. Ernzerhof, M.E. John P. Perdew, Kieron Burke, *Phys. Rev. Lett.* 78, 3865–3886 (1996).
- [35] J. M. S. Pablo Ordejón, Emilio Artacho, *Phys. Rev. B.* 53, R10441(R) (1996).
- [36] P.O. and D.S.-P. José M. Soler, Emilio Artacho, Julian D. Gale, Alberto García, Javier Junquera, *J. Phys. Condens. Matter.* 14, 2745–2779 (2002).
- [37] S.L. Mayo, B.D. Olafson, W.A. Goddard III, *J. Phys. Chem.* 94, 8897–8909 (1990).
- [38] A. K. Rappe, C.J. Casewit, K.S. Colwell, W. a Goddard, W.M. Skiff, *J. Am. Chem. Soc.* 114, 10024–10035 (1992).
- [39] S.K. Nath, *J. Phys. Chem. B.* 107, 9498–9504 (2003).
- [40] J. J. Potoff, J.I. Siepmann, *AIChE J.* 47, 1676–1682 (2001).
- [41] A.P. Terzyk, S. Furmaniak, P.A. Gauden, P. Kowalczyk, *Adsorpt. Sci. Technol.* 27, 281–296 (2009).
- [42] S.S. Han, D. Jung, J. Heo, *J. Phys. Chem. C.* 117, 71–77 (2013).
- [43] M. Shadman, S. Yeganegi, M.R. Galugahi, *J. Iran. Chem. Soc.* 13, 207–220 (2016).
- [44] W. Smith, T. R. Forester, *J. Mol. Graph.* 14, 136–141 (1996).